11

Charge Transport and Electrical Switching in Composite Biopolymers

Gabriel Katana[1] and Wycliffe Kipnusu[2]
[1]*Physics Department, Pwani University College, P.O. Box 195 Kilifi,*
[2]*Institute of Experimental Physics I, University of Leipzig, 04103 Leipzig,*
[1]*Kenya*
[2]*Germany*

1. Introduction

Polymers are long chain macromolecules made up of many repeating units called monomers. They are found in nature and can also be made synthetically. Natural/bio polymers are considered to be environmental benign materials as opposed to synthetic polymers. Research geared toward producing innocuous products from biopolymers has intensified. Improved understanding of properties of biopolymers allows for the design of new eco-friendly materials that have enhanced physical properties and that make more efficient use of resources. Biopolymers also have the advantage of being biodegradable and biocompatible. They are therefore of interest for application in advanced biomedical materials, for instance tissue engineering, artificial bones or gene therapy (Eduardo et al., 2005). Other possible fields of applications are related to electrical properties, making this class of materials attractive for potential uses in electronic switches, gates, storage devices, biosensors and biological transistors (Finkenstadt & Willett 2004). Plant biopolymers constitute the largest pool of living organic matter most of which can be attributed to four distinct classes of organic compounds; lignin, cellulose, hemicellulose and cuticles. Cuticles are mainly made up of polymethylenic biopolymers which include cutin and suberin. Cutin-containing layers are found on the surfaces of all primary parts of aerial plants, such as stems, petioles, leaves, flower parts, fruits and some seed coats. In addition, cutin may be found on some internal parts of plants such as the juice-sacs of citrus fruits (Heredia, 2003). Composition, structure and biophysical data of plant cuticles have recently been reviewed (Jeffree, 2003; Pollard et al. 2008; and Dom´ınguez et al., 2011) and will only be mentioned briefly. The main constituents of cutin are esterified fatty acids hydroxylated and epoxy hydroxylated with chain lengths mostly of 16 and 18 carbon atoms. It also contains some fraction of phenolic and fluvanoid compounds.

2. Charge transfer mechanism in biopolymers

Several biopolymers have well documented properties as organic semiconductors (Eley et al., 1977; Leszek et al., 2002; Radha & Rosen, 2003; Mallick & Sakar, 2000; Lewis & Bowen, 2007; Ashutosh & Singh 2008). DNA-based biopolymer material possesses unique optical and electromagnetic properties, including low and tunable electrical resistivity, ultralow

optical and microwave low loss, organic field effect transistors, organic light emitting diodes (LED) (Hagen et al., 2006). Nonlinear optical polymer electro-optic modulators fabricated from biopolymers have demonstrated better performance compared to those made from other materials (Piel et al., 2006).Naturally occurring Guar gum biopolymer chemically modified with polyaniline exhibits electrical conductivity in the range of 1.6×10^{-2} S/cm at room temperature (Ashutosh & Singh 2008). Mallick & Sakar (2000) investigated electrical conductivity of gum arabica found in different species of Acacia babul [*Acacia Arabica*] (Boutelje, 1980) and found that its electrical properties are similar to that of synthetic conducting polymer doped with inorganic salt and are proton conducting in nature.

Charge transport in biomolecular materials takes place mainly through two processes: Super exchange transport and hopping transport. Super exchange is a chain mediated tunneling transport. In this process electrons or holes are indirectly transferred from a donor to acceptor group through an energetically well- isolated bridge, where the bridge orbitals are only utilized as coupling media. In the hopping mechanism, the electron temporarily resides on the bridge for a short time during its passing from one redox center to the other, but in the super-exchange, the conjugated bridge only serves as a medium to pass the electron between the donor and acceptor (Tao et al., 2005). Tunnelling is a process process that decays exponentially with the length of the molecule. A simple tunneling model assumes a finite potential barrier at the metal-insulator interface. It describes free electron flow for a short distance into the sample from the metal contact. At low voltages the charge transfer is described by Simmons relations (DiBenedetto et al., 2009) but at higher applied voltages the tunneling is determined by Fowler-Nordheim process. Superexchange process can either be coherent or non-coherent. Coherent tunneling process is whereby a charge carrier moves from a donor to acceptor fast enough such that there is no dephasing by nuclear motions of the bridge (Weiss et al., 2007). Consequently, charges do not exchange energy with the molecules. However this process does not take place at significantly long distances. Incoherent superexchange on the other hand is a multi-step process in which a localized charge carrier interacts with phonons generated by thermal motion of the molecules (Singh et al., 2010)

As opposed to superexchange, hopping transport in biopolymers is a weakly distance dependent incoherent process. Generally superexchange is a short range transfer of charges in a spatial scale of a few Å while hopping transport takes place over a longer distance greater than 1nm. The exact mechanism of tunneling and hopping is not fully understood but it is known to be influenced by several factors. First, type of charge carriers in biopolymers which can either be holes, electrons or even polarons influences charge transport. Hole transfer is initiated by photo-oxidation of the donor groups attached to the terminus of the molecule whereas electron transfer occurs by chemical reduction of the acceptor group. A direct reduction of the molecule in contact with the metal electrode occurs when the voltage is applied. The interplay between donor acceptor and coupling fluctuation in biological electron transfer has also been observed (Skourtis et al., 2010). Secondly, band structure and hoping sites also influence charge transport. Although there are no band structures in biomolecules, energy gaps exist due to different hybridized electronic states. These energy gaps provide hopping sites through which charges propagate. Finally, conformation and spatial changes for the conducting state may overlap and hence create hopping sites as described by variable range hopping (Shinwari et al., 2010). Variable range hopping mainly describes transport mechanism in solid-state materials, but has also been observed in biopolymers (Mei Li et al., 2010). Similar to superexchange, electron hopping in

biopolymers is a multi-step process. According to this mechanism, the overall distance between primary electron donor and final electron acceptor is split into a series of short electron transfer steps. The essential difference is the existence of bridge units (oxidized or reduced species) that function as relays system and the fact the hopping process has a weak distance dependence (Cordes & Giese, 2009).Both of the two processes can take place at the same time and have been observed by several experimental groups. Treadwaya et al. (2002) noted that DNA assemblies of different lengths, sequence, and conformation may allow tunneling, hopping, or some mixture of the two mechanisms to actually dominate.

From measurements that probed changes in oxidized guanine damage yield with response to base perturbations, Armitage et al. (2004) noted that charge transfer through base-base of DNA molecules takes place through hopping via the π-π bond overlap. Tao et al. (2005) reported electron hopping and bridge-assisted superexchange charge transfer between donor and an acceptor groups in peptide systems. The charge and dipole of the peptide play an important role in the electron transfer (Amit et al., 2008). Galoppini & Fox (1996) demonstrated the effect of electric field generated by the helix dipole on electron transfer in Aib-rich α helical peptides and found out that other than the effect from secondary structure (α helix and β sheet), dipole and hydrogen bonding, the solvent also has a marked influence on the study of the electron transfer. Due to complexity of peptides, the importance of individual amino acids in controlling electron transfer is not yet understood in detail.

Similar studies in proteins have concluded that electron transfer can occur across hydrogen bonds and that the rate of such transfer is greatly increased when the electron motions are strongly coupled with those of the protons (Ronald et al., 1981). While studying energy transport in biopolymers, Radha & Rossen (2003) suggested, based on the experimental results, that a soliton in biopolymers is an energy packet (similar to the "conformon" which is the packet of conformational strain on mitochondria) associated with a conformational strain localized in region much shorter than the length of a molecule. It was also noted by the same group that as the soliton (localized curvature) moves on the polymer, it could trap an electron and drag it along. This mechanism may be important in understanding charge transport in biological molecules, where curvatures abound. Studies on charge transport in ethyl cellulose- chloranil systems have also been done, (Khare et al., 2000) where the space charge limited current (SCLC) was found to be the dominant mode of electrical conduction at high field in these systems.

Mechanisms leading to charge conduction in metal-polymer-metal configuration have been the subject of intensive study in the past two decades. Much of these studies have focused on doped and undoped synthetic polymers where the commonly discussed high-field electronic conduction mechanism for various films are Fowler-Nordheim tunneling, Poole-Frenkel (P-F), Richardson-Schottky (R-S) thermionic emissions, space charge limited conduction and variable range hopping. Based on the same sample geometry it is reasoned that the mechanism mentioned above could also contribute to detectable current flow in biopolymers sandwiched between metal electrodes. These mechanisms are discussed hereunder and in section 5, experimental results based on cutin biopolymer are presented and discussed in reference to the charge transport mechanism mentioned above.

2.1 Fowler-Nordheim tunneling

In Fowler-Nordheim tunneling the basic idea is that quantum mechanical tunneling from the adjacent conductor into the insulator limits the current through the structure. Once the carriers have tunneled into the insulator they are free to move within the material.

Determination of the current is based on the Wentzel, Kramers and Brillouin (WKB) approximation from which Eq. (1) is obtained.

$$J_{FN} = \chi_{FN} E^2 \exp\left[-\frac{4}{3}\frac{\sqrt{2m^*}}{q\hbar}\frac{\left(q\varphi_B\right)^{3/2}}{E}\right] \tag{1}$$

where J_{FN} is the current density according to Fowler -Nordheim, χ_{FN} is the Fowler Nordheim constant, E is the electric field, m^* is the effective mass of the tunneling charge, $\hbar$ is a reduced plancks constant, q is the electron charge and ϕ_B is the potential barrier height at the conductor/insulator interface. To check for this current mechanism, experimental I-V characteristics are typically plotted as $\ln(J/E^2)$ vs $1/E$, a so-called Fowler-Nordheim plot. Provided the effective mass of the insulator is known, one can fit the experimental data to a straight line yielding a value for the barrier height.

2.2 Field emission process

Whereas Fowler-Nordheim tunneling implies that carriers are free to move through the insulator, it cannot be the case where defects or traps are present in an insulator. The traps restrict the current flow because of a capture and emission process. The two field emission charge transport process that occur when insulators are sandwiched between metal electrodes are Poole-Frenkel and Schottky emission process. Thermionic (schottky) emission assumes that an electron from the contact can be injected into the dielectric once it has acquired sufficient thermal energy to cross into the maximum potential (resulting from the superposition of the external and the image-charge potential). If the sample has structural defects, the defects act as trapping sites for the electrons. Thermally traped charges will contribute to current density according to Poole-Frenkel emission. They are generally observed in both organic and inorganic semiconducting materials. Poole-Frenkel effect is due to thermal excitation of trapped charges via field assisted lowering of trap depth while Schottky effect is a field lowering of interfacial barrier at the blocking electrode. Expression for Poole-Frenkel and Schottky effects are given in Eq. (2) and (3) respectively.

$$J_{PF} = J_{PFO} \exp[(\beta_{PF} E^{1/2}) / kT] \tag{2}$$

$$J_S = J_{SO} \exp[(\beta_S E^{1/2}) / kT] \tag{3}$$

J_{SO} and J_{PFO} are pre-exponential factors, β_S is the Schottky coefficient, β_{PF} is the Poole-Frenkel coefficient, and E is the electric field. The theoretical values of Schottky and Poole-Frenkel coefficient are related by Eq.(4):

$$\beta_S = \left(e^3 / 4\pi\varepsilon\varepsilon_0\right) = \beta_{PF} / 2 \tag{4}$$

where q is electron charge, ε is relative permittivity, ε_0 permitibity in free space

2.3 Space charge limited current

For structures where carriers can easily enter the insulator and freely move through the insulator, the resulting charge flow densities are much higher than predicted by Fowler-Nordheim tunneling and Poole-Frenkel mechanism. The high density of these charged

carriers causes a field gradient, which limits the current density and the mechanism is then referred to as space charge limited current. Starting from the basic Gauss's law in one-dimension, assuming that the insulator contains no free carriers if no current flows the expression for the space charge limited current can be obtained as shown in Eq. (5)

$$J = \frac{9\varepsilon\mu V^2}{8d^3} \tag{5}$$

where J is current density, ε is relative permittivity,μ is charge mobility, V is applied voltage and d is electrode spacing. Space charge limited current results from the fact that when the injected carrier concentration exceeds the thermal carrier concentration, the electric field in the sample becomes very non-uniform, and the current no longer follows Ohm's law.

2.4 Variable-range hopping mechanism

Charge conduction in semiconducting polymers is thought to take place by hopping of charge carriers in an energetically disordered landscape of hopping sites (Meisel et al., 2006). The variable-range hopping (VRH) conduction mechanism originally proposed by Mott for amorphous semiconductors (Mott & Davis, 1979) assuming a phonon-assisted hopping process has also been observed in conducting polymers and their composites at low temperature (Ghosh et al., 2001; Luthra et al., 2003; Singh et al., 2003). Bulk conductivity of conducting polymers depends upon several factors, such as the structure, number and nature of charge carriers, and their transport along and between the polymer chains and across the morphological barriers (Long et al., 2003). When the phonon energy is insufficient (low temperature), carriers will tend to hop larger distances in order to locate in sites which are energetically closer than their nearest neighbours. Eq. (6) gives the DC conductivity based on the VRH conduction model.

$$\sigma = \frac{\sigma_0}{\sqrt{T}} \exp[-\left(\frac{T_d}{T}\right)^{1/4}] \tag{6}$$

where the pre- exponential factor σ_0 is given by Eq.(7)

$$\sigma_0 = \frac{q^2 v_{ph}}{2(8\pi k)^{1/2}} \left[\frac{N_{(EF)}}{\gamma}\right]^{1/2} \tag{7}$$

and q is the electron charge, k is the Boltzmann's constant, v_{ph} is the typical phonon frequency obtained from the Debye temperature ($\approx 10^{13}$ Hz), γ is the decay length of the localized wave function near the Fermi level and $N_{(EF)}$ is the density of states at the Fermi level. The characteristic Mott temperature T_d, as shown in Eq.(8) corresponds to the hopping barrier for charge carriers (also known as the pseudo-activation energy) and measures the degree of disorder present in the system.

$$T_d = 18.11 \frac{\gamma^3}{kN_{(EF)}} \tag{8}$$

Two other Mott parameters, the variable range hopping distance (R_{VRH}) and hopping activation energy (W) are given by Eq. (9) and (10) respectively

$$R_{VRH} = \left[\frac{9}{8\pi\gamma kTN_{(EF)}} \right]^{1/4} \tag{9}$$

$$W = \frac{3}{4\pi R^3 N_{(EF)}} \tag{10}$$

3. Electrical switching mechanism in bioploymers

Biomolecules often have sensitive bio-active sites that can change under external stimuli such as temperature, light, electrical signals, PH and chemical/biochemical reactions of their environs. Such switchable biomolecules are of tremendous usefulness in diverse areas including biological, medical and bio-electronic technology. Most research groups in this field are interested in investigating new class of switchable biological systems albeit the field is still at its infancy stage. Chu et al. (2010) reported electro-switchable oligopetides as a function of surface potential. Oligolysine peptides exhibit protonated amino side chain at PH-7 providing the basis of switching ''ON'' and ''OFF'' of the biological activity on the surface upon application of negative potential. Switching initiated by PH changes has been observed in other biomolecules and biopolymers (Zimmermann et al., 2006). Biomolecular motors of actomyosin experience rapid and reversible on-off switching by thermal activation (Mihajlovi et al., 2004). The most optimistic approach of integrating photo switchable biomolecules into opto-electronic devices is provided by highly photo sensitive bacteriorhodopsin. This molecule has shown remarkable photo sensitive switching of its electrical properties that mimic conventional Gate transistors (Roy et al., 2010; Pandey, 2006; Qun et al., 2004). Bottom-up approach toward building optical nano-electronic devices is also feasible with the discoveries of switchable photoconductivity in even the smallest structures such as quantum dots of cross-linked ligands (Lilly et al., 2011).

Electrical switching in biomolecules has wider applications in electronic industry. However, a lucid understanding of microscopic switching mechanism in these biological systems is still an outstanding challenge. In most investigations probing electrical switching in organic molecules, an external electrical signal is applied to the sample sandwiched between metal electrodes. Many materials have been reported to show hysteretic impedance switching where a system in its high impedance state (OFF) is switched by a threshold voltage into a low impedance state (ON) and remains in the ON state even with the reversal of applied voltage. This phenomenon is also known as resistive switching. Switching mechanism depend on whether the contribution comes from thermal, electronic, or ionic effects (Waser et al., 2007). Resistive switching is generally dependent on number of mobile charges, their mobility and the average electric field. In the case where the current is highly localized within a small sample area, filamental conduction take place (Scott et al., 2007). This simply involves formation of metallic bridge connecting the two electrodes. Filamental conduction accounts for negative differential resistance (NDR) model which is the basis of many molecular switching processes (Ren et al., 2010). Although this model was originally applied to inorganic materials, it can also explain resistive switching in organic samples (Tseng et al., 2006). The model assumes a trap- controlled channel where tunnelling take place in between chains of metallic islands. Similarly a decrease in electron transport channels and weak coupling between electrodes and the contact molecule causes NDR switching behaviour. Electric field induced switching mechanism is common in literature (Waser et al., 2007). In

general terms, built up of space charges trapped within the sample due to presence of defects create a field which is large enough to cause flow of mobile charge carriers. This phenomenon is sometimes called coulomb blockade (Tang et al., 2005). At high electric fields, charges are injected by Fowler-Nordheim tunnelling and subsequently trapped. As a result, electrostatic barrier character of the structure is modified and so is its resistance.

The most insightful switching mechanism in biomolecules is the redox process and the formation of charge transfer complex through donor-acceptor coupling. Aviram et al. (1988) suggested that electron- proton motion within hemiquinones molecules that comprised of catechol and o-quinone, molecules between two contacts switch the molecules to low impedance (ON) state due to the formation of semiquinones fee radicals. When an electron is injected into the molecules from the metal contact, it is gained by an electron acceptor molecule. An electron donor molecule then transfers the electron to the opposite contact thus allowing flow of charge.

The present chapter discusses structural characteristics (by use of Fourier Transform Infra-Red spectroscopy and Atomic Force Microscopy). Electrical conduction in cuticular membranes of Nandi flame (*Spathodea campanulata*, P. Beav) seeds hereafter referred just as cuticles. Fig. 1 shows the cuticle also presented still attached to the seed. The cuticles are thin (about 2 μm), translucent and very light. They are adapted to wind dispersion of the seeds.

4. Structural characterization

4.1 Fourier transform infra Red (FTIR) spectroscopy

Fig.2 shows the Fourier Transform Infra Red (FTIR) spectroscopy of the pristine cuticle. The samples were first annealed at 350K for 12 hrs before measurement. The wide band at 3348 cm^{-1} which has been observed in many other cuticular membranes (Bykov, 2008) is assigned to O-H stretching vibration. It is caused by presence of alcoholic and phenolic hydroxyl groups involved in hydrogen bonds. Methylene is the most repeated structural unit in the cutin biopolyester (Jose, et al., 2004) and these shows up in the spectra band around 2300 cm^{-1}. The band at 2916 cm is assigned to C-H asymmetric and symmetric stretching vibrations of methoxyl groups. Absorption around 1604 cm^{-1} and 1427 cm^{-1} are assigned to the stretching of C=C bonds and the stretching of benzenoid rings. Absorption bands in the range 1300-1150 cm^{-1} are related to asymmetric vibration of C-O-C linkages in ester to esters or phenolic groups. Fig. 3 show the infra red (IR) spectra of cuticle compared with the spectra of other biopolymers.

Fig. 1. Thin and translucent cuticle attached to the Nandi flame seed

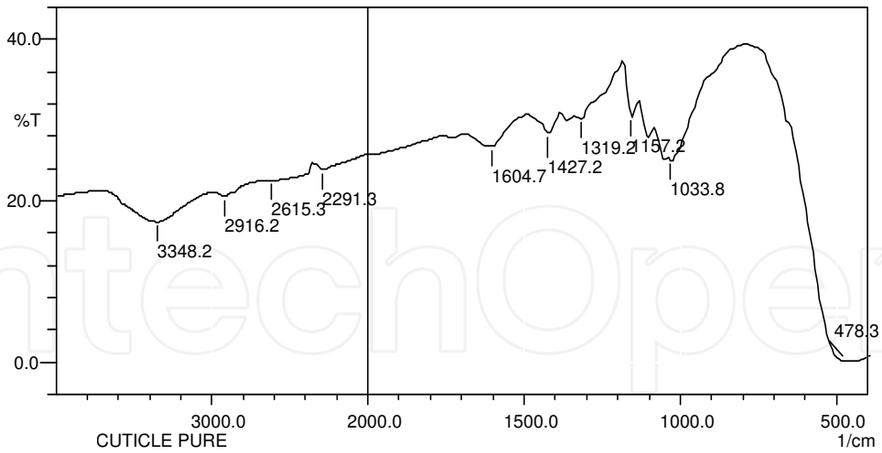

Fig. 2. FT-IR spectrum of pristine cuticle

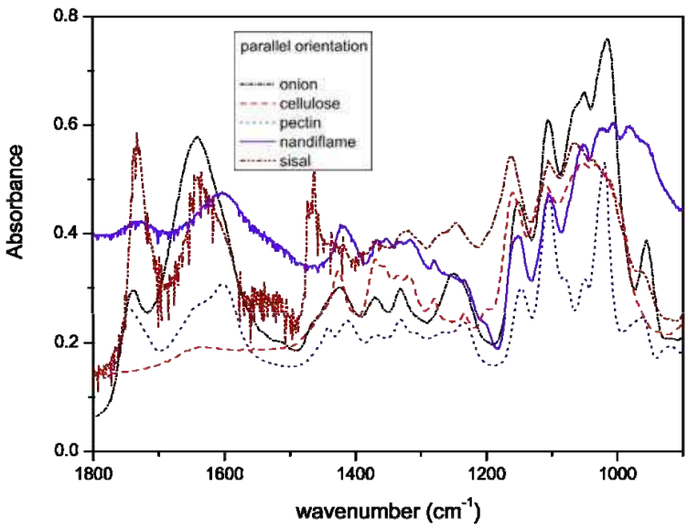

Fig. 3. Comparison of IR spectrum of Nandi flame cuticle with those of other biopolymers

4.2 Atomic force microscopy (AFM)

The AFM scans (Fig. 4) shows that NFSC has a highly oriented surface topography. The AFM permits measurement of the distance variations in the surface of the sample by use of two pairs of cursors. The cursors can be made to scale the surface in nanometer (nm) or micrometer (μm).

The interstitial region between the ridges represented in the dark area in Fig. 4 represents cavities in the membrane with a diameter of about 0.5nm. It is important to note that molecular basal spacing (cavities) in the range of 0.4-0.5nm has also been observed from molecular dynamic simulations of a cutin oligomer (Domınguez et al., 2011) and is attributed to the distance between the methylene groups of oligomeric chain. The presence of such cavities is a typical property of amorphous cross-linked polymers and may be important in explaining the interaction between cutin and endogenic low-molecular weight compounds such as phenolics and flavonoids.

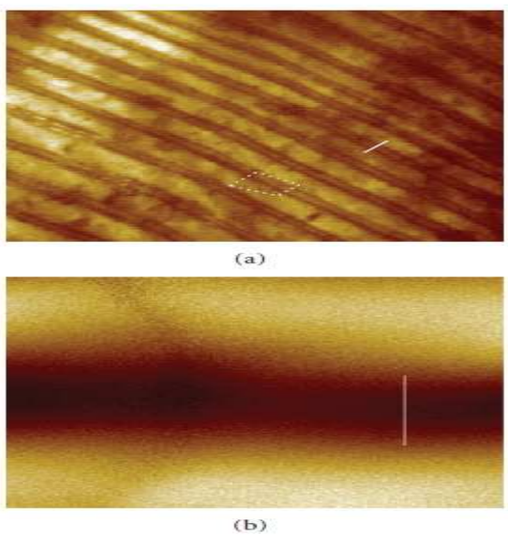

Fig. 4. AFM topographic scans showing surface structure of the cuticle; (a) is a map from the scan on a larger area of about 3×10^5 square pixels (b) is a scan on a single pixel of about 2.5×10^6 nm^2. Doted lines on (a) represents the region shown by (b). Scale bars ~ 0.5nm.Taken from (Kipnusu et al., 2009).

5. Electrical characterization and charge transport mechanism

This section discusses electrical characteristics of the cuticle samples. Current-voltage (I-V) data measured as a function of annealing temperature, irradiation and pooling temperature was used in analyzing the electrical characteristics .Samples were separately annealed and irradiated before electrode coating was done. When annealing, cuticles were placed inside a temperature-controlled furnace, which was fitted inside an electrical shielded cage of a Lindberg/Blue Tube Furnace of model TF55035C. Samples were annealed at various temperatures of 320K, 350K and 400K for a constant period of 12hrs each. Irradiation of the sample was done with He-Ne laser beam of wavelength 632.8nm in a dark room each for a different period of 10minutes, 30minutes, and 60minutes. Electrode coating on the film of pristine, pre-annealed and pre-irradiated samples was done by using quick drying and highly conducting Flash-Dry silver paint obtained from SPI Supplies (USA). A mask of a circular aperture of 0.56 cm diameter was used while coating to ensure uniformity in size of coated surface. Circular aluminum foil of the same diameter was placed on freshly coated surface such that the sample was sandwiched between two aluminum electrodes. These metal-sample-metal sandwiches were left to dry at room temperature for a period of 24hrs to ensure that there was good ohmic contacts between aluminum electrode and the sample. The same Flash-Dry Silver paint was used to connect thin wires onto the aluminum electrodes. When measuring I-V at different temperatures, a sample sandwiched between aluminium electrodes was placed inside the Lindbarg/Blue Tube Furnace and temperature varied in steps of 5K between 350K and 500K at constant electric fields of 0.75V/cm, 1.50V/cm 2.25V/cm, 3.00V/cm, and 3.75V/cm.

Fig. 5(a) shows the I-V characteristics of pristine and annealed samples. These indicate clearly that there was electrical switching and memory effect in the cuticle samples. At

certain threshold voltage, V_{th} current rises rapidly by an order of 2. There are two distinct regions for the increasing voltage. At low voltages the log I versus log V plots are approximately linear with a slope of 1; while at higher voltages, above a well-defined threshold voltage V_{th}, the plots are again approximately linear with a slope of 2.04 ± 0.07. These plots therefore show that at low voltages, OFF-state, current follows ohms law but after switching to ON-state at higher voltages, current follows a power law dependence given by $I \alpha V^n$ where $n = 2.04 \pm 0.07$ obtained from linear regression fitting parameters where the standard deviation was shown as 0.03 and coefficient of correlation as 0.0001. This shows that the ON-state region is governed by Space charge limited current (SCLC) controlled by single trapping level, the injecting carrier concentration dominating the thermally generated carriers. During the switching process the current increases appreciably leading to a local increase in temperature (Collines et al., 1993). The current does not follow the same path on decreasing applied electric field hence indicating that the samples exhibit memory switching that is not erased by annealing. The threshold voltage V_{th} for pristine samples is 5.0+0.5 volts. The width of V_{th} or transition voltage during switching from OFF to ON states is about 1.0 V. Inset of Fig 5 (a) shows non-uniform increase of V_{th} with the increase in annealing temperature and tends to attain a plateau at higher annealing temperature. Decrease in magnitude of the negative dielectric anisotropy during annealing is a major reason for the increase in V_{th} for the annealed samples (Katana& Muysoki, 2007). Annealing polymeric films at different temperatures causes structural changes which affects electrical conductivity. Annealing temperature increases grain size in the polymer films causing many changes in the electrical and other properties (Leszek et al., 2002). Threshold voltage V_{th} for pristine cuticles is higher than V_{th} reported for some synthetic polymers; PMMA (1.6V), PS (4.5V), Phthalocyanine (0.3V), 2,6-(2,2-bicyanovinyl) pyride (5.01V), Langmuir-Blodgett (1.0V) (Katana& Muysoki, 2007; Otternbacher et al., 1991; Xue et al., 1996; Sakai et al., 1988).

Fig. 5(b) shows I-V curves for cuticle samples that were pre-irradiated with laser light of wavelength 632.8nm for different duration of time. Just as noted for the annealed samples, I-V curves for irradiated samples shows electrical switching and memory effect with V_{th} that increases with the increase in irradiation time (see inset Fig. 5b). Increasing time of irradiation increases electrical conductivity. The increase in conductivity for irradiated samples can be attributed to dissociation of primary valence bonds into radicals. Dissociation of C-C and C-H bonds leads to degradation and cross linking which improves electrical conductivity (Ashour et al., 2006). Exposure of polymers to ionizing radiation produces charge carriers in terms of electron and holes which may be trapped in the polymer matrix at low temperatures (Feinheils et al., 1971). If the original conductivity is small, then the presence of these carriers produces an observable increase in conductivity of the polymer. Irradiation of polymers results in excitations of its molecules and creation of free electrons and ions that migrate through the polymer network till they are trapped. The electronic and ionic configurations created, cause changes in the electric conductivity. In the study of effect of gamma irradiation on the bovine Achilles tendon (BAT) collagen, Leszek et al. (2002) reported changes in electrical conductivity that is dose dependent. Higher concentration of free radicals generated by irradiation of collagen created charge carriers that increased electrical conductivity.

Fig.5(c) shows I-V curves of the cuticles obtained at different poling/measurement. These curves show that electrical current increases as measurement temperature increase. This is due to thermal excitation of the trapped charges across the potential barrier. The curves also show that forward bias characteristics have two regions which are typical examples of ohmic conduction for voltages below V_{th} (OFF-state) and a space charge limited current (SCLC) for voltages above V_{th} (ON-state).. Increase in temperature facilitates diffusion of ions in the space charge polarization. Thermal energy may also aid in overcoming the activation barrier for orientation of polar molecules in the direction of the field. Charge carrier generation and transport in mitochondrial lipoprotein system has been investigated by electrical conductivity and the results show that increase in temperature causes a transition in conductivity where steady state conduction is correlated with chain segmental reorientations of phospholipid moiety below the transition and with an interfacial polarization process above it (Eley et al., 1977).

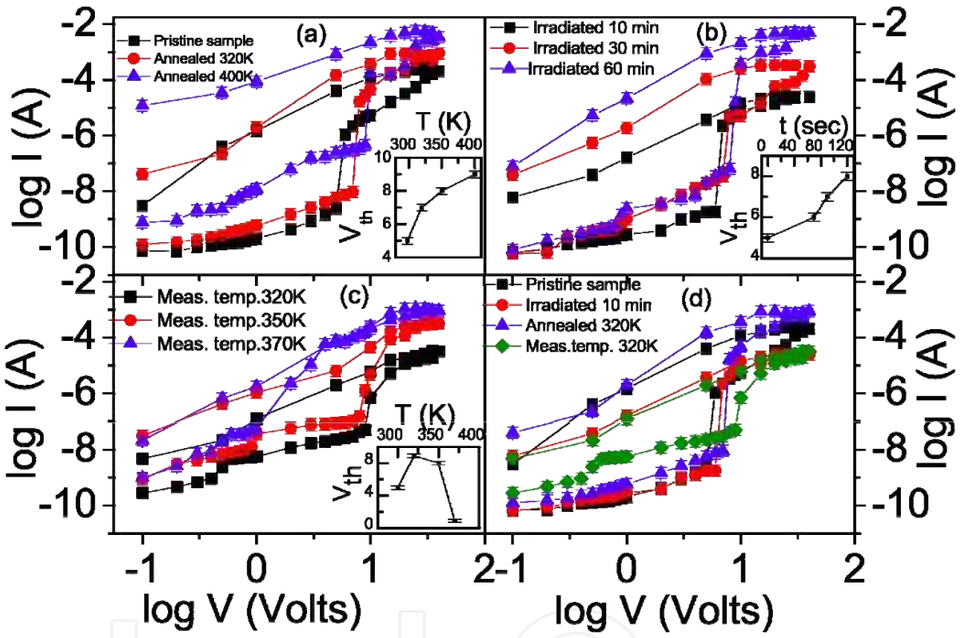

Fig. 5. I-V curves of the pristine cuticles and cuticles treated at different conditions. (a) pristine & samples pre-annealed at 320K and 400K for 12hrs each. (b) pristine & samples pre- irradiated with laser light of wavelength 632.8nm for the duration shown in the legends.(c) pristine samples measured at different temperatures. The insets in (a), (b) and (c) show variation of threshold voltage as a function of the annealing temperature, irradiation time, and measurement temperature respectively. (d) shows combined curves with the conditions shown in the legends.

V_{th} rapidly decreases with the increase in measurement temperature and that switching and memory effect almost disappears at higher temperatures (370K). This is due to the fact that the V_{th} decreases and that the gap between current in the forward bias and reverse bias in the ON-state region almost closed up such that the forward bias current nearly folllows the same path as the reverse bias current which indicates a loss of memory.

It is difficult to draw unambiguous conclusion from Fig.5 (d) because all the three imposed conditions affect conductivity in unique ways and also depends on duration of annealing, irradiation and the measurement temperature. However it is worthy mentioning that at measurement temperature of 320K conductivity is higher than conductivity of presitne samples at low electric field (OFF state). This observation is however reversed at higher electric fields where conductivity of pristine samples is higher.

Switching and memory behavior can be attributed to the fact that external electric field triggers embedded molecules with ridox centers hence creating some traps. Switching mechanism in these systems is by quantum interference of different propagation parts within the molecules which involve permutation of Lowest Unoccupied Molecular Orbitals ($LUMO_{+1}$) and Highest Occupied Molecular Orbitals ($HOMO_{-1}$)-the frontier orbitals. To get electric field induced switching effect, the relative energies of HOMO (localized on the donor group) and LUMO (localized on the acceptor group) must be permuted (Aviram et tal., 1988). This switching model supposes that both the permuting orbitals are initially doubly degenerate resulting to what is referred to as frontier orbitals. In the absence of electric field $HOMO_{-1}$ is localized on the acceptor group and $LUMO_{+1}$ on the donor group. When the external field is applied, electron orbitals are "pulled" towards the acceptor group reducing the HOMO-LUMO gap of frontier orbitals and the switching and hybridization between $HOMO_{-1}$ and $LUMO_{+1}$ takes place. While the strength of the field increases, the HOMO-LUMO gap in the molecular spectrum becomes smaller and the HOMO, $HOMO_{-1}$ and LUMO orbital split into the HOMO-LUMO gap and hence become delocalized. Electrical switching can also in part be explained by formation of quinoid and semiquinone structures from phenolic compounds accompanied by redox reactions. The quinoid form is planar, and is highly conjugated compared to phenyl groups. Changes in bond length and rotation of benzene ring during formation of quinoid structure results in activation barriers which are considered to be the origin of the temperature dependence conductance. Details of this explanation is found in Kipnusu et al. (2009b)

Fowler-Nordheim emission current is given in equation (1). To check for this current mechanism, experimental *I-V* data for annealed samples of NFSC were analyzed by potting $\ln(J/E^2)$ versus $1/E$. Four plots were made to represent different regime with different levels of measured current (Fig.6). Fowler-Nordheim tunneling mechanism is confirmed by straight lines with negative slopes given by; $4\left(2m^*\right)^{1/2}/3q\hbar(q\varphi_B)^{3/2}$ where m^* is the effective mass of the tunneling charge, q is the electron charge, $\hbar$ is a reduced planck constant, and ϕ_B is the barrier height expressed in eV units. Fig.6 shows that Fowler-Nodheim curves for low and high fields forward bias and low filed reverse bias were quite non-linear or had positive slopes therefore ruling out possibility of Fowler-Nordheim mechanism in these regimes. However in Fig.6 (d) the curves are relatively linear with negative slopes. This is the high fields' regime of the reverse bias where the current increased with decreasing voltage (see Fig.5). Making an assumption that m^* equals the electron rest mass (0.511MeV), and using the slope obtained from linear fits of Fig. 6 (d),the potential barrier height at the Al/cuticle junction is found to be 11.28 eV and 1.13 eV for pure samples and samples annealed at 400K respectively. Vestweber et al. (1994) noted that if the barrier height exceeds 0.3 eV tunnel process prevail with the consequence that high anodic fields are required in order to attain high current densities. It can therefore be concluded that Fowler-Nordheim quantum mechanical tunneling was responsible for the

surge of current with decreasing field since the model assumes that once the carriers have tunneled into the insulator they are free to move within the material.

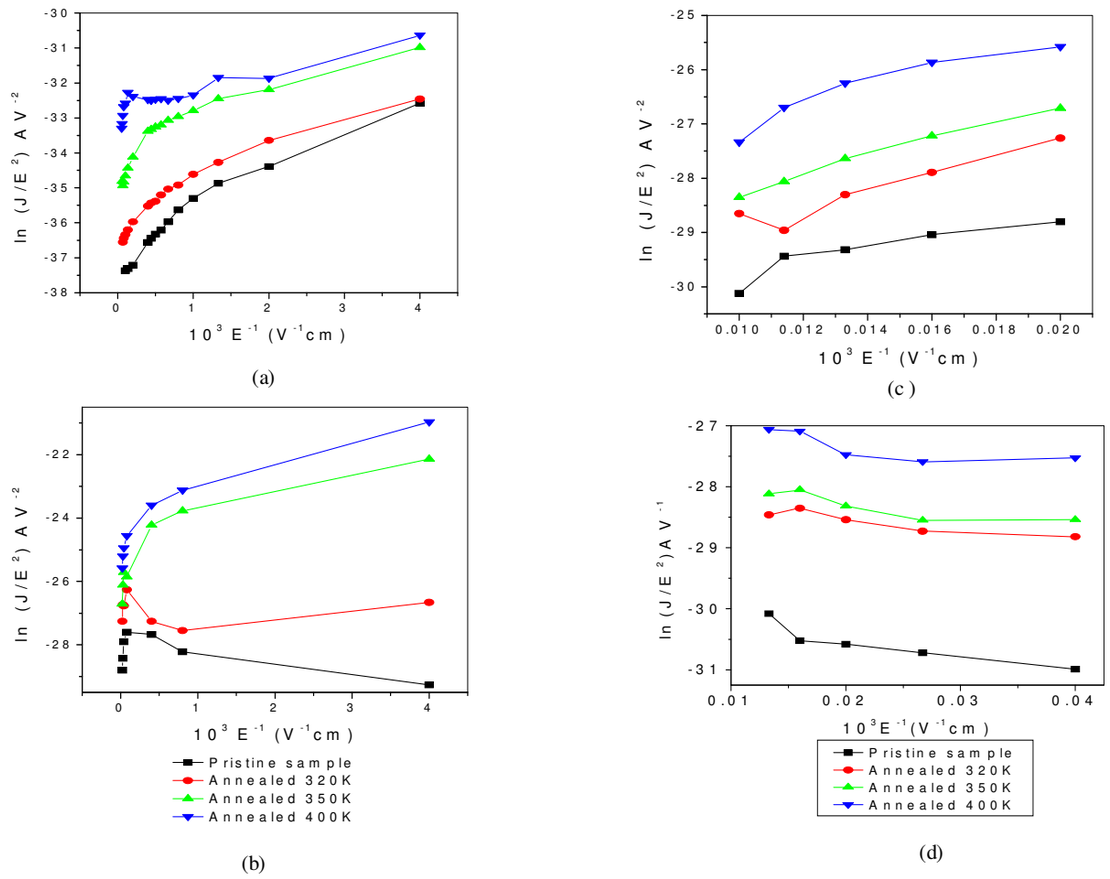

Fig. 6. Fowler-Nordheim curves: (a) Forward bias at low electric field (b) Reverse bias at low electric field (c) forward bias at high electric field and (d) reverse bias at high electric field.

Fig. 7. shows curves of current density versus square root of electric (*ln J versus* $E^{1/2}$) in the low field for forward bias regime. These curves neither support conduction mechanism by Poole-Frenkel nor Schottky emissions which predict linear graphs of *ln J versus* $E^{1/2}$ with positive slopes. Fig.8 shows linear fittings of *ln J versus* $E^{1/2}$ for forward and reverse bias at high fields (10^4 -10^5 V/cm). The current levels in the reverse bias are higher than forward bias. This behaviour may be interpreted either in terms of Poole-Frenkel effect which is due to thermal excitation of trapped charges via field assisted lowering of trap depth or by Schottky effect which is a field lowering of interfacial barrier at the blocking electrode (Deshmukh et al. 2007). The expressions for these processes are given in Eq.(2) and (3) respectively. Schottky coefficient (β_S) and Poole-Frenkel coefficient (β_{PF}) are related as shown in Eq. (4). Using the value of static dielectric permitivity (ε) of 3.0, (determined from dielectric spectroscopy) theoretical values of β_S and β_{PF} obtained from Eq. (4) are 3.51×10^{-24} J $V^{1/2}$ $m^{1/2}$ and 7.01×10^{-24} J $V^{1/2}$ $m^{1/2}$ respectively. Experimental values of β obtained from the slopes of plots of *lnJ versus* $E^{1/2}$ (Fig.8) at different temperatures are listed in Table 1. The standard deviation and coefficient of linear correlation were obtained as 0.34 and 0.005

respectively. The large discrepancy in experimental values of β listed in Table 1 and theoretical values of β_S and β_{PF} leads to a conclusion that current transport mechanism in our samples governing the high field at a temperature range of 320K-370K cannot be explained in terms of Shottky or Poole-Frenkel emission.

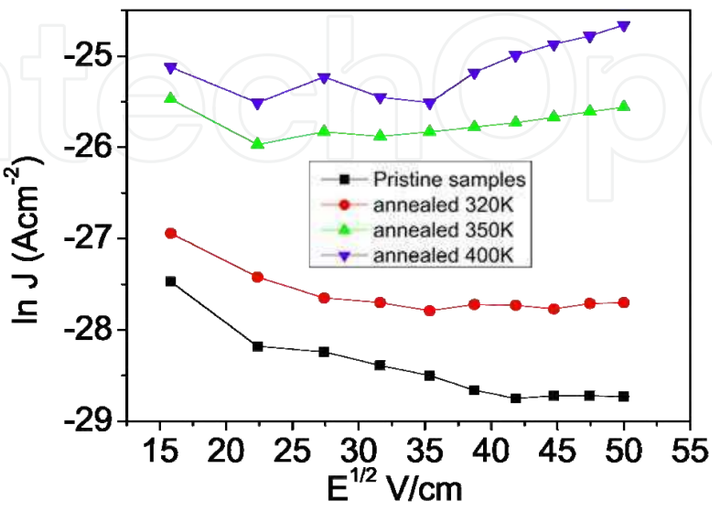

Fig. 7. Semi logarithmic plots of *ln J* versus $E^{1/2}$ for the low field of 225-2500 V/cm at a temperature range of 320K-400K

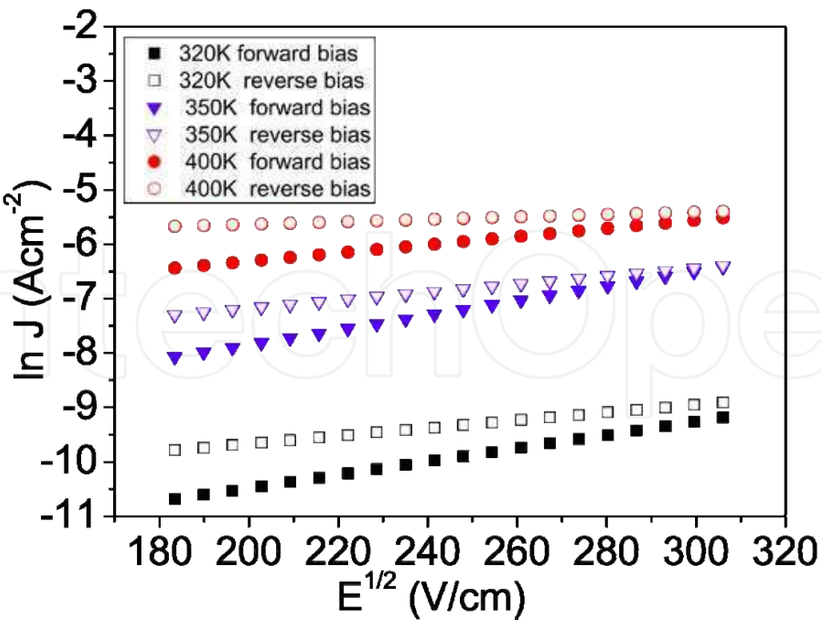

Fig. 8. Semi logarithmic plots of *ln J* versus $E^{1/2}$ for the high field of 3.2×10^{4}- 9.8×10^{5}V/cm in forward and reverse biases at temperature range of 320K-400K

To analyze the effect of temperature on conductivity of the samples, Arrhenious curves ($\log\sigma$ vs 10^3/T) for different polarizing fields (0.75kV/cm, 1.50kV/cm, 2.25kV/cm,3.00kV/cm, and 3.75kV/cm) were plotted (Fig. 9) using the Arrhenius Eq. (11);

$$\sigma = \sigma_0 \exp\left(\frac{-E_a}{kT}\right) \tag{11}$$

where σ is conductivity, σ_o the pre-exponential factor, E_a the activation energy, k is Boltzmann's constant, and T is temperature in Kelvin. Conductivity was obtained from the Eq. (12);

$$\sigma = \frac{I}{V}\frac{d}{A} \tag{12}$$

where I is measured current, V is measured Voltage, d is the thickness of the samples (≈4.0 ×10^{-4} cm), and A is the electrode active area (circular electrode of diameter 0.56cm was used). Initial increase in conductivity at low temperature is due to the injection of charge carriers directly from the electrodes. The increase in conductivity at selectively low field is due to the increase in the magnitude of the mean free path of the photon (Sangawar et al., 2006). At high temperatures, the increase in conductivity may be attributed to softening of the polymer which causes the injected charge carrier to move more easily into the volume of the polymer giving rise to a large current. Increased conductivity at higher temperatures could also be due to thermionic emission across the barrier potential.

Temperature (K)	Experimental $\beta \times 10^{-23}$ ($Jm^{1/2}$ $V^{1/2}$) values	
	Forward bias	Reverse bias
320	5.65 ± 0.12	3.17± 0.12
350	6.31 ± 0.14	3.56± 0.12
370	3.44± 0.04	0.93± 0.02

Table 1. Values of β obtained from experimental data

Variable range hopping mechanism predicts linear dependence of $\ln(\sigma T^{1/2})$ versus $T^{-1/4}$ with negative slope (Fig.9, inset b). The Mott parameters- T_d, γ and $N(E_F)$- are determined from equations 6 to 10 using the slope and intercept values of the plots in inset (b) of Fig. 9 and assuming a phonon frequency ((υ_{ph}) of 10^{13} s^{-1}. Other Mott parameters, the hopping distance R and average hopping energy W are determined from Eq. (9) and Eq. (10) respectively. Mott parameters from this calculation are listed in Table 2. Table 3 shows the variations of the Mott parameters with temperature in our samples. It is evident from Table 3 that $\gamma R > 1$ and $W > kT$, which agrees with Mott's condition for variable range hopping. It can therefore be concluded that the main conduction mechanism in NFSC is the variable range hopping.

Mott parameters	Value
T0 (K)	4.58×10^{10}
N(EF) ($eV^{-1}cm^{-3}$)	9.04×10^{19}
α (cm^{-1})	3.0×10^{8}
R (cm)	1.44×10^{-7}
W (eV)	0.89

Table 2. Mott parameters at temperature range of (320-440K)

T (K)	R (cm^{-1})	W (eV)	kT (eV)	γR
300	1.54×10^{-7}	0.72	0.026	41.6
350	1.49×10^{-7}	0.81	0.030	40.1
400	1.44×10^{-7}	0.89	0.034	38.7
450	1.39×10^{-7}	0.98	0.039	37.6

Table 3. Variation of Mott parameters at temperature range of 300-450K

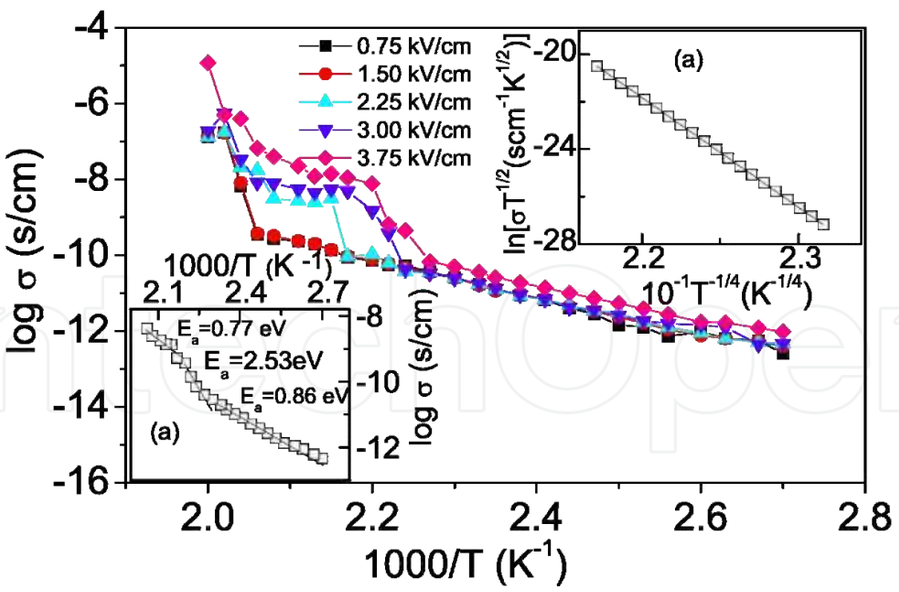

Fig. 9. Arrhenius plots showing variation of σ *vs 1/T* at different electric fields. Inset (a) average Arrhenius plot showing activation energy at low and intermediate temperature ranges. Inset (b) plot of ln $(\sigma T^{1/2})$ versus $(T^{-1/4})$ within a temperature of 350K-440K and average electric field of 2.25Kv/cm.

Degree of localization of the carriers in the trap states is indicated by $\gamma R>1$ which shows that the charges are highly localized. Table 3 also shows that when the temperature decreases, the average hopping energy W decreases and the average hopping distance R increases, supporting the fact that when the phonon energy is insufficient (low temperature), carriers will tend to hop larger distances in order to locate in sites which are energetically closer than their nearest neighbours.

6. Conclusion

Current-Voltage characteristics of the cuticles, as a function of irradiation, annealing, and temperature, show electrical switching with memory effect. The threshold voltage increases with irradiation time and annealing temperature but it decreases with increase in measurement temperature. The threshold voltage of the annealed and irradiated samples ranges between 6-8 volts. Electrrical conduction in the OFF state follows Ohms' law but changes to space charge limited current after switching to ON state. A combination of Fowler-Nordheim field emission process and redox processes are responsible for electrical switching of the samples. Conduction at low temperatures takes place by variable range hopping mechanism. Since this biomaterial is biodegradable and is also considered to be biocompatible and immunologically inert, it has high potential in biomedical applications. It can be used in making contact eye lenses, scaffolds in tissue engineering, and in controlled release of drugs. Most notably, due to its switching properties, its use in the design of biosensors utilizing ion channels is very feasible.

7. References

Amit, P.;Watson, R; Lund, P; Xing, Y.; Burke, K.; Yufan H,; Borguet, E.; Achim, C; & Waldeck D. (2008). Charge Transfer through Single-Stranded Peptide Nucleic Acid Composed of Thymine Nucleotides. *J.Phys. Chem*., Vol. 112, pp. 7233-7240

Armitage N., Briman M., & Gruner M. (2004). charge transfer and charge transport on the double helix. *Phys.stat. sol.*(b) Vol.241(1), pp. 69-75

Ashour, H., Saad, M., & Ibrahim, M. (2006). Electrical Conductivity for Irradiated, Grafted Polyethylene and Grafted Polyethylene with Metal Complex. *Egypt. J. Solids,* Vol. 29(2), pp. 351-362.

Ashutosh, T., & Singh, S. (2008). Synthesis and characterization of biopolymer-based electrical conducting graft copolymers. *J. Appl. Polym. Sci*, Vol.108(2), pp.1169-1177.

Aviram A., Joachim C. & Pomerantz M. (1988). Evidence of Switching and Rectification by a Single Molecule Effected with a Scanning Tunneling Microscope. *Chem. Phys. Lett.*, Vol.146(6), pp. 490-495

Boutelje, J. (1980). *Encyclopedia of world timbers, names and technical literature*. (Enc wTimber).p234

Bykov, I. (2008). *Characterization of Natural and Technical Lignins using FTIR Spectroscopy.* Master thesis, Lulea University of Technology, Lulea

Chun L.; Parvez, Y. Iqbal,Y.; Marzena A.; Lashkor, M.;Preece, J. & Mendes,P.(2010). Tuning Specific Biomolecular Interactions Using Electro-Switchable Oligopeptide Surfaces.*Adv. Funct. Mater.*, Vol.20, pp.2657–2663

Collins, R. & Abass, A. (1993). Electrical switching in Au-PbPc-Au thin film sandwich devices. *Thin Solid Films,* Vol.235, pp.22-24

Cordes, M. & Giese B. (2009). Electron transfer in peptide and proteins. Chemical society review, Vol. 38, pp. 892-901

Deshmukh, S., Burghate, D., Akhare, V., Deogaonkar, V., & Deshmukh, P. (2007). Electrical conductivity of polyaniline doped PPV-PMMA polymer blends. *Bull.Matter. Sci.* Vol. 30(1), pp.51-56

DiBenedetto, S.; Facchetti, A.; Rather, M.; & Marks, T. (2009). Molecular self-assembly monolayers and multilayers for organic and unconventional inorganic thin films transistor applications. Advanced materials, Vol.21, pp. 1407-1433

Dom´ınguez, E.; Alejandro, J.; Guerrero, H. & Heredia, A. (2011). The biophysical design of plant cuticles: an overview. *New Phytologist,* vol. 189, pp. 938–949

Eduardo, R., Margarita, D., & Pilar, A. (2005). Functional biopolymer nanocomposites based on layered solids. *J. Mater. Chem.* 15: 3650–3662 DOI: 10.1039/ b505640n

Eley, D., Lockhart, N., & Richardson, C. (1977). Electrical properties and structural transitions in the mitochondrion. *Journal of Bioenergetics and Biomembranes,* Vol.9(5), pp.289-301

Feinleib J., DeNeufville J., Moss S., and Ovshinsky S. (1971). Rapid reversible light-induced crystallization of amorphous semiconductors. *Applied Physics Letters*, Vol.18, pp. 254–257

Finkenstadt, V. & Willett, J. (2007). Preparation and characterization of electroactive biopolymers. *Macromolecular symposia* ISSN 0258-0322.

Galoppini, E, and Fox M. (1996). Role of dipoles in peptide electron transfer. *J.Am. Chem. Soc.* Vol.118, pp. 2299-2300.

Ghosh, M., & Meikap, A., Chattopadhyay ,S. and Chatterjee, S. (2001) Low temperature transport properties of Cl-doped conducting polyaniline. *J. Phys. Chem. Solids,* Vol.62, pp. 475–84

Gmati, F., Arbi, F., Nadra, B., Wadia, D. and Abdellatif, B. (2007). Comparative studies of the structure, morphology and electrical conductivity of polyaniline weakly doped with chlorocarboxylic acids. *J. Phys.: Condens. Matter,* Vol. 19, pp.326203

Hagen, J.; Li, W.; & Steckl, J. (2006). Enhanced emission efficiency in organic light-emitting diodes using deoxyribonucleic acid complex as an electron blocking layer. *Applied Physics Letters,* Vol. 88, pp. 171109(1-3)

Heredia,A. (2003). Biophysical and biochemical characteristics of cutin, a plant barrier biopolymer, *Biochimica et Biophysica Acta* Vol. 1620 pp. 1 – 7

Jose J. B., Matas, A. J., & Heredia, A. (2004). Molecular characterization of the plant biopolyester cutin by AFM and spectroscopic techniques. *Journal of Structural Biology.* Vol. 147, pp.179–184

Katana, G. & Musyoki, A. (2007). Fabrication and performance testing of gas sensors based on organic thin films. *J. Polym. Mater.* Vol.24 (4), pp.387-394

Khare, P., Pandey, R., and Jain P . (2000) .Electrical transport in ethyl cellulose –chloranil system. *Bull.Mater. Sci.* Vol.23 (4), pp.325-330

Kipnusu, W.; Katana, G.;Migwi, M.; Rathore, I.; & Sangoro J.(2009). Charge Transport Mechanism in Thin Cuticles Holding Nandi Flame Seeds, *International Journal of Biomaterials*, doi:10.1155/2009/548406

Kipnusu, W.; Katana, G.;Migwi, M.; Rathore, I.; & Sangoro J.(2009). Electrical Switching in Thin Films of Nandi Flame Seed Cuticles. *International Journal of Polymer Science*, doi:10.1155/2009/830270

Leszek, K., Ewa, M., & Feliks, J. (2002). Changes in the Electrical Conductivity of the - irradiated BAT collagen. *Polish J Med Phys & Eng*. Vol.8(3), pp.157-164

Lewis,T.&Bowen, P. (2007). Electronic Processes in Biopolymer Systems. Electrical Insulation, IEEE Transactions, El- Vol.19 (3),pp. 254-256

Lilly, G.; Whalley,A.; Grunder, S.; Valente,C.; Frederick, M.; Stoddart, J & Weiss, E. (2011). Switchable photoconductivity of quantum dot films using cross-linking ligands with light-sensitive structures. Journal of Materials Chemistry, in press match 2011 DOI: 10.1039/c0jm04397d

Long, Y., Chen, Z., Wang, N., Zhang, Z., & Wan, M. (2003). Resistivity study of polyaniline doped with protonic acids, *Physica* B Vol.325, pp.208–213

Luthra, V., Singh, R., Gupta, S., & Mansingh, A. (2003). Mechanism of dc conduction in polyaniline doped with sulfuric acid *Curr. Appl. Phys.* Vol.3, 219–222.

Mallick, H., & Sakar, A. (2000). An experimental Investigation of electrical conductivity in biopolymers.*Bull.mater.sci*.Vol.23.4, pp. 319-324

Mei Li, Z.; Turyanska, L.; Makarovsky, O.;Amalia Patan, A.; Wenjian Wu, W.; & S Mann, S. (2010). Self-Assembly of Electrically Conducting Biopolymer Thin Films by Cellulose Regeneration in Gold Nanoparticle Aqueous Dispersions. *Chem. Mater*. ,Vol. 22, pp. 2675–2680

Meisel, D., Pasveer, W., Cottaar, I., Tanase, I., Coehoorn, R., Bobbert, P., Blomp,W., De Leeuw D., & Michels, M. (2006). Charge-carrier mobilities in disordered semiconducting polymers: effects of carrier density and electric field. *phys. stat. sol*. (c) Vol.3, (2), pp. 267– 270.

Mihajlovića, G.; Brunet, N.; Trbović, J.; Xiong, P.; Molnár, S.; & Chase,P. (2004).All-electrical switching and control mechanism for actomyosin-powered nanoactuators, *Appl. Phys. Lett*., Vol. 85, (6), pp. 1060-1062

Mott, N. & Davis, E. (1979). *Electronic Processes in Non-Crystalline Materials* (Oxford: Clarendon) p 157–60

Ottenbacher, D.,Schierbaum, K., & Gopel, W. (1991). Switching effect in metal/ Phthalocyanine/metal sandwich structures. *Journal of molecular electronics* Vol.7(7),pp.9-84

Pandey, P.C. (2006). Bacteriorhodopsin—Novel biomolecule for nano devices. *Analytica Chimica Acta*,Vol. 568, pp. 47–56

Priel, A.; Ramos, A.; Tuszynski, J.; & Horacio F.; Cantiello, H. (2006). A Biopolymer Transistor: Electrical Amplification by Microtubules. *Biophysical Journal* Vol. 90 , pp. 4639–4643

Pollard, M.; Beisson, F.;Li,and , Y.; & Ohlrogge,J. (2008). Building lipid barriers: biosynthesis of cutin and suberin. *Trends in Plant Science*, vol. 13, (5), pp. 236–246

Qun, L.;, Stuart, J.; Birge, R.; Xub, J.; Andrew Stickrath, A.; & Bhattacharya, P. (2004).Photoelectric response of polarization sensitive bacteriorhodopsin films. *Biosensors and Bioelectronics* ,Vol.19, pp.869–874

Radha, B., & Rossen, D. (2003). Nonlinear elastodynamics and energy transport in biopolymers. ArXiv:nlin.PS/ 0304060 vI

Ren,Y.; Chen,.;K.; He, J.; Tang, L.; Pan, A.; Zou, B.; & Zhang, Y. (2010). Mechanically and electrically controlled molecular switch behavior in a compound moleucular device. *Applied Physics Letters*, Vol 97, pp. 103506 (1-3)

Ronald, P., Peter, R., and Albert S. (1981). Water structure-dependence charge transport in proteins. *Proc.Natl. Acad. Sci USA*. Vol.78 (1), pp.261-265

Roy, S.; Prasad, M.; Topolancik, J.; & Vollmer, F . (2010). All-optical switching with bacteriorhodopsin protein coated microcavities and its application to low power computing circuits. *Journal of Applied Physics*,Vol. 107, pp. 053115(1-9)

Sakai, K., Matsuda H., Kawada H., Eguchi K., & Nakagiri T. (1998). Switching and memory phenomena in Langmuir-Blodgett films. *Appl. Phys. Lett.* Vol.53(14), pp.1274-1276

Sangawar, V., Chikhalikar P., Dhokne R., Ubale A., & Meshram S. (2006). Thermally stimulated discharge conductivity in polymer composite thin films. *Bull.Mater.Sci.* 29: 413-416

Singh,M.; Graeme, B.; Allmang, M.; (2010). Polaron hopping in nano-scale poly(dA)-poly(dT) DNA. *Nanoscale Res.Lett*. Vol. 5, pp. 501-504

Singh, R., Kaur A., Yadav K., and Bhattacharya D. (2003). Mechanism of dc conduction in ferric chloride doped poly(3-methyl thiophene) *Curr. Appl. Phys.* 3: 235–238

Shinwari, M.; Deen,M.; Starikov,E and Gianaurelio, C. (2010). Electrical conductance in biological molecules. Advance functional materials, Vol. 20. Pp. 1865-1883

Skourtis, S.; Waldeek, D. & Beratan, D. (2010). Fluctuation in biological and bioinspired electron transfer reaction. *Annual Review Phys. Chem.* March 2010, Vol. 61, pp. 461-485

Tang, W., Shi, H., Xu, G., Ong, B., Popovic, Z., Deng, J., Zhao, J. & Rao, G. (2005), Memory Effect and Negative Differential Resistance by Electrode- Induced Two-Dimensional Single- Electron Tunneling in Molecular and Organic Electronic Devices. *Advanced Materials*, 17: 2307–2311

Tao, L., Erfan, A., & Heinz-Bernhard, K. (2005). Peptide electron transfer. *Chem..Eur.J.,* Vol.11, pp.5186-5194.

Treadway , C.; Hill, M.G . & Barton, J.K . (2002). Charge transport through a molecular π-stack: double helical DNA.*Chemical Physics*, Vol. 281, pp.409–428

Tseng,R.; Ouyang, J.; Chu, C.; Huang, J.; & Yanga, Y.(2006). Nanoparticle-induced negative differential resistance and memory effect in polymer bistable light-emitting device. *Applied Physics Letters*, Vol. 88, pp. 123506 (1-3)

Waser, R. & Aono, M. (2007). Nanoionics-based resistive switching memories, *Nature materials*, Vol. 6, pp. 833-840

Weiss E.; Kriebel,J.; Maria-Anita Rampi, M.; & Whitesides, G. (2007). The study of charge transport through organic thin films: mechanism, tools and applications. *Philosophical Transaction of the Royal Society A.* Vol, 365 pp. 1509-1537

Xue, Z., Ouyang, M.,Wang, K., Zhang, H., and Huang, C. (1996). Electrical switching and memory phenomena in the Ag-BDCP thin film. *Thin Solid Films,* Vol.288, pp. 296-299

Zimmermann, R.;Osaki, T.;ller, T.; Gauglitz, G.; Dukhin, S. & Werner, C. (2006).Electrostatic Switching of Biopolymer Layers. Insights from Combined Electrokinetics and Reflectometric Interference. *Anal. Chem.*, Vol. 78, pp. 5851-5857

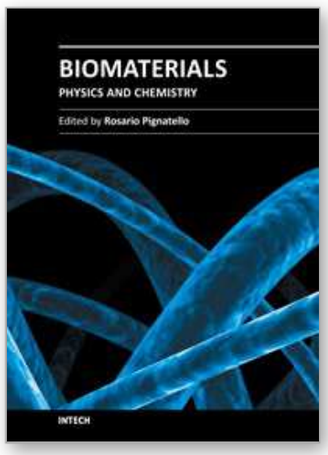

Biomaterials - Physics and Chemistry

Edited by Prof. Rosario Pignatello

ISBN 978-953-307-418-4
Hard cover, 490 pages
Publisher InTech
Published online 14, November, 2011
Published in print edition November, 2011

These contribution books collect reviews and original articles from eminent experts working in the interdisciplinary arena of biomaterial development and use. From their direct and recent experience, the readers can achieve a wide vision on the new and ongoing potentialities of different synthetic and engineered biomaterials. Contributions were selected not based on a direct market or clinical interest, but based on results coming from very fundamental studies. This too will allow to gain a more general view of what and how the various biomaterials can do and work for, along with the methodologies necessary to design, develop and characterize them, without the restrictions necessarily imposed by industrial or profit concerns. The chapters have been arranged to give readers an organized view of this research area. In particular, this book contains 25 chapters related to recent researches on new and known materials, with a particular attention to their physical, mechanical and chemical characterization, along with biocompatibility and hystopathological studies. Readers will be guided inside the range of disciplines and design methodologies used to develope biomaterials possessing the physical and biological properties needed for specific medical and clinical applications.

InTech Europe
University Campus STeP Ri
Slavka Krautzeka 83/A
51000 Rijeka, Croatia
Phone: +385 (51) 770 447
Fax: +385 (51) 686 166
www.intechopen.com

InTech China
Unit 405, Office Block, Hotel Equatorial Shanghai
No.65, Yan An Road (West), Shanghai, 200040, China
中国上海市延安西路65号上海国际贵都大饭店办公楼405单元
Phone: +86-21-62489820
Fax: +86-21-62489821

IntechOpen